

---

---

# <sup>68</sup>Ga-Citrate PET of Healthy Men: Whole-Body Biodistribution Kinetics and Radiation Dose Estimates

Sami Suilamo<sup>1,2</sup>, Xiang-Guo Li<sup>3-5</sup>, Petteri Lankinen<sup>6,7</sup>, Vesa Oikonen<sup>3</sup>, Tuula Tolvanen<sup>1,7</sup>, Pauliina Luoto<sup>3,7</sup>, Riikka Viitanen<sup>3</sup>, Antti Saraste<sup>3,7,8</sup>, Marko Seppänen<sup>7,9</sup>, Laura Pirilä<sup>10,11</sup>, Ulla Hohenthal<sup>12</sup>, and Anne Roivainen<sup>3,5,7</sup>

<sup>1</sup>Department of Medical Physics, Turku University Hospital, Turku, Finland; <sup>2</sup>Department of Oncology and Radiotherapy, Turku University Hospital, Turku, Finland; <sup>3</sup>Turku PET Centre, University of Turku, Turku, Finland; <sup>4</sup>Department of Chemistry, University of Turku, Turku, Finland; <sup>5</sup>InFLAMES Research Flagship Center, University of Turku, Turku, Finland; <sup>6</sup>Department of Orthopaedics and Traumatology, Turku University Hospital and University of Turku, Turku, Finland; <sup>7</sup>Turku PET Centre, Turku University Hospital, Turku, Finland; <sup>8</sup>Heart Center, Turku University Hospital, Turku, Finland; <sup>9</sup>Department of Clinical Physiology and Nuclear Medicine, Turku University Hospital, Turku, Finland; <sup>10</sup>Department of Rheumatology and Clinical Immunology, Division of Medicine, Turku University Hospital, Turku, Finland; <sup>11</sup>Department of Medicine, University of Turku, Turku, Finland; and <sup>12</sup>Department of Infectious Diseases, Division of Medicine, Turku University Hospital, Turku, Finland

<sup>68</sup>Ga-citrate has one of the simplest chemical structures of all <sup>68</sup>Ga-radiopharmaceuticals, and its clinical use is justified by the proven medical applications using its isotope-labeled compound <sup>67</sup>Ga-citrate. To support broader application of <sup>68</sup>Ga-citrate in medical diagnosis, further research is needed to gain clinical data from healthy volunteers. In this work, we studied the biodistribution of <sup>68</sup>Ga-citrate and subsequent radiation exposure from it in healthy men. **Methods:** <sup>68</sup>Ga-citrate was prepared with an acetone-based radiolabeling procedure compliant with good manufacturing practices. Six healthy men (age 41 ± 12 y, mean ± SD) underwent sequential whole-body PET/CT scans after an injection of 204 ± 8 MBq of <sup>68</sup>Ga-citrate. Serial arterialized venous blood samples were collected during PET imaging, and the radioactivity concentration was measured with a  $\gamma$ -counter. Urinary voids were collected and measured. The MIRD bladder-voiding model with a 3.5-h voiding interval was used. A model using a 70-kg adult man and the MIRD schema was used to estimate absorbed doses in target organs and effective doses. Calculations were performed using OLINDA/EXM software, version 2.0. **Results:** Radioactivity clearance from the blood was slow, and relatively high radioactivity concentrations were observed over the whole of the 3-h measuring period. Although radioactivity excretion via urine was rather slow (biologic half-time, 69 ± 24 h), the highest decay-corrected concentrations in urinary bladder contents were measured at the 90- and 180-min time points. Moderate concentrations were also seen in kidneys, liver, and spleen. The source organs showing the largest residence times were muscle, liver, lung, and heart contents. The heart wall received the highest absorbed dose, 0.077 ± 0.008 mSv/MBq. The mean effective dose (International Commission on Radiological Protection publication 103) was 0.021 ± 0.001 mSv/MBq. **Conclusion:** PET imaging with <sup>68</sup>Ga-citrate is associated with modest radiation exposure. A 200-MBq injection of <sup>68</sup>Ga-citrate results in an effective radiation dose of 4.2 mSv, which is in the same range as other <sup>68</sup>Ga-labeled tracers. This suggests the feasibility of clinical studies using <sup>68</sup>Ga-citrate imaging in humans and the possibility of performing multiple scans in the same subjects across the course of a year.

**Key Words:** biodistribution; <sup>68</sup>Ga-citrate; PET; pharmacokinetics; radiation dose

**J Nucl Med 2022; 63:1598–1603**  
DOI: 10.2967/jnumed.122.263884

**F**or PET imaging, <sup>68</sup>Ga is a transition metal that can be used as <sup>68</sup>Ga-citrate or <sup>68</sup>Ga-chloride and also in its chelated forms with biomolecules (e.g., chelator-conjugated peptides). <sup>68</sup>Ga-labeled pharmaceuticals are frequently used in nuclear medicine and can conveniently be manufactured with kits and fully automated commercially available devices (1). <sup>68</sup>Ga-citrate is one such <sup>68</sup>Ga-radiopharmaceutical that has entered the clinical trial stage, and its use in PET is based on Ga<sup>3+</sup> uptake and transportation mechanisms. Ga<sup>3+</sup> is considered an analog of Fe<sup>3+</sup> and binds to transferrin and other biomolecules in vivo. Although only a few human studies using <sup>68</sup>Ga-citrate PET have been performed (2–13), <sup>68</sup>Ga-citrate has already been shown to be a sensitive and specific PET tracer for the imaging of infection and inflammation, including inflammatory bowel disease (3), bone infection (4), intraabdominal infection (5), and prosthetic joint infection (12). In addition, we recently observed unexpectedly high <sup>68</sup>Ga-citrate accumulation in atherosclerotic lesions in patients with *Staphylococcus aureus* bacteremia (8). Furthermore, patients with high-grade glioma, hepatocellular carcinoma, and prostate cancer have been imaged with <sup>68</sup>Ga-citrate according to the hypothesis that Ga<sup>3+</sup> uptake should increase in these tumors because of upregulated activity of transferrin receptor (7,9–11). Evidence from clinical and preclinical investigations (7,14,15) suggests that <sup>68</sup>Ga-citrate has potential in several clinical applications and that further research is warranted.

The purpose of this clinical study was to determine the biodistribution of intravenously administered <sup>68</sup>Ga-citrate in healthy male volunteers. This information will help to determine the optimal PET protocol for <sup>68</sup>Ga-citrate imaging of inflammatory and infectious diseases and cancer. The whole-body imaging should allow identification of those organs that are most exposed to ionizing radiation and allow calculation of the dose absorbed by each organ.

---

Received Jan. 28, 2022; revision accepted Mar. 7, 2022.  
For correspondence or reprints, contact Anne Roivainen (anne.roivainen@utu.fi).  
Published online Mar. 10, 2022.  
COPYRIGHT © 2022 by the Society of Nuclear Medicine and Molecular Imaging.

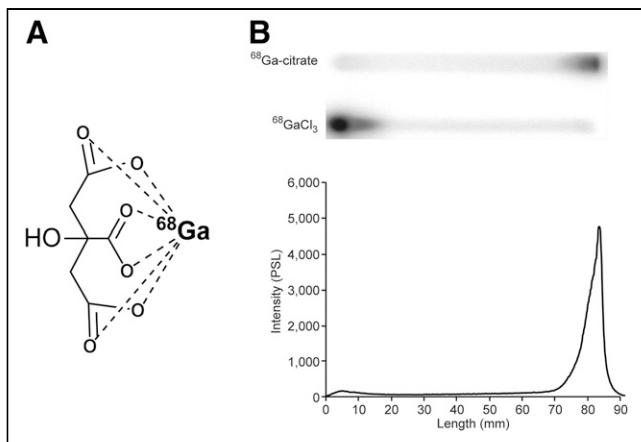


**FIGURE 1.** (A) Chemical structure of  $^{68}\text{Ga}$ -citrate. (B) Quality control of  $^{68}\text{Ga}$ -citrate with instant thin-layer chromatography developed using methanol/acetic acid (9:1, v/v) as mobile phase and visualized and quantified by autoradiography.

## MATERIALS AND METHODS

### Chemicals and Reagents

All chemicals were purchased from commercial sources and were of reagent, analytic, ultrapure, or European Pharmacopeia grade.

### Preparation of $^{68}\text{Ga}$ -Citrate

$^{68}\text{Ga}$ -citrate (Fig. 1A) was produced according to an established protocol (3). Aqueous hydrochloric acid (0.1 M, 6 mL) was used to elute  $^{68}\text{Ga}$  radioactivity from a  $^{68}\text{Ge}/^{68}\text{Ga}$  generator (IGG-100, 1,850 MBq; Eckert and Ziegler Isotope Products), and the  $^{68}\text{Ga}$ -eluate was passed through a cation-exchange cartridge (Strata X-C; Phenomenex Inc.). The retained  $^{68}\text{Ga}$  was eluted into a reaction vial with acidified acetone (800  $\mu\text{L}$ , containing 0.02 M HCl and 3.25% water). The acetone was removed by evaporation for 4 min at  $110^\circ\text{C}$ , and sodium citrate buffer (4 mL) was added. After 4 min, the reaction mixture was sterile-filtered into an end-product vial and diluted with saline (9 mg/mL, 6 mL). Radiochemical purity was measured by instant thin-layer chromatography with methanol/acetic acid (9:1, v/v) as a mobile phase.

### Subjects

Six healthy male volunteers (age,  $41 \pm 13$  y; weight,  $75 \pm 4$  kg; height,  $177 \pm 4$  cm) participated in this trial.  $^{68}\text{Ga}$ -citrate was injected via a catheter inserted into an antecubital vein, and blood samples were drawn through another catheter inserted into the contralateral arm.

Before the start of this clinical trial, approvals were obtained from the joint Ethics Committee of the University of Turku and Turku University Hospital, as well as from the Finnish Medicines Agency. Full informed consent was obtained in writing from all subjects beforehand. This study is registered at ClinicalTrials.gov (NCT01951300).

Questionnaires were used to assess the absence of significant medical, neurologic, and psychiatric history and of any history of alcohol or drug abuse. In addition, routine blood tests, electrocardiography, a physical examination, and a review of medical history were performed for each subject.

### PET/CT Imaging

The biodistribution of  $^{68}\text{Ga}$ -citrate was imaged using a Discovery 690 PET/CT scanner (GE Healthcare). This scanner combines 64-slice CT with PET acquired using 24 rings of lutetium-yttrium-orthosilicate detectors, which provide 47 imaging planes with an axial field of view of 15.7 cm. A low-dose CT scan for attenuation correction and anatomic reference was acquired before the PET scan, using a voltage of

120 kV and current of 10 mA. Whole-body PET acquisitions were made 1, 5, 10, 20, 30, 90, and 180 min after an intravenous injection of  $204 \pm 8$  MBq of  $^{68}\text{Ga}$ -citrate. The acquisition times per bed position were 20, 30, 65, 65, 120, 240, and 240 s, respectively. The scanning at 90 min after injection included 14 bed positions covering the range from the head to the toes, whereas all other scans used only 8 bed positions covering the range from the head to mid thighs.

PET images were reconstructed using a time-of-flight 3D VUE Point algorithm (GE Healthcare) with 2 iterations, 24 subsets, and a postprocessing filter of 6.4 mm in full width at half maximum. Scatter correction, random counts, and dead-time corrections were all incorporated into the reconstruction algorithm. The final matrix size was  $192 \times 192 \times 47$  voxels. The plane thickness of the PET scanner was 3.27 mm, and the axial spatial resolution for 3-dimensional mode was 4.74 mm in full width at half maximum at a 1-cm offset from the center of the field of view (16).

### Blood and Urine Measurements

Serial arterialized (the arm was heated with a wrapped heating pad) venous blood samples were collected into heparinized tubes at 1, 5, 10, 20, 30, 60, 90, 180, and 240 min after the injection of  $^{68}\text{Ga}$ -citrate. The radioactivity of the whole blood was measured with an automatic  $\gamma$ -counter (1480 Wizard 3'; EG&G Wallac). Plasma was separated by centrifugation (2,100g for 5 min at  $4^\circ\text{C}$ ), and the plasma radioactivity was measured. The plasma concentration at baseline ( $C_0$ ) was estimated by fitting a monoexponential function to the plasma concentrations collected between 5 and 30 min.

The subjects were asked to urinate during 2 breaks in the PET imaging session and again after the session. The mean times for urination were 61 min after injection, 163 min after injection, and 218 min after injection. Urinary voids were collected, the total volume was measured, and a 2.5-mL sample was taken for radioactivity measurement with a VDC 405 dose calibrator (Veenstra Instruments).

### Distribution Kinetics and Radiation Dose Estimates

Eclipse software (version 13.6; Varian Medical Systems) was used to define the radioactivity concentrations of the source organs at different time points. The source organ volumes either were defined on CT images or were the volumes of the organs of the reference man (17).

Residence times in source organs were calculated from area under the time-activity curves. The curves were defined by fitting a sum of 2 exponential functions. The MIRD bladder-voiding model (18) with a 3.5-h voiding interval was used. A model with a 70-kg adult man and MIRD schema (19) was used to estimate the absorbed doses in the target organs and the effective doses. Calculations were performed using OLINDA/EXM software, version 2.0. In addition, OLINDA 1.0 results were calculated.

## RESULTS

### Radiochemistry

The manufactured  $^{68}\text{Ga}$ -citrate fulfilled all the product quality specifications (Supplemental Table 1; supplemental materials are available at <http://jnm.snmjournals.org>) for clinical use. The radiochemical purity was at least 95%, pH was in the range of 3.0–7.0, and the acetone content was no more than 0.5%. An example instant thin-layer chromatography plot used to determine radiochemical purity is shown in Figure 1B.

### Biodistribution and Biokinetics

Whole-body dynamic PET/CT imaging data were obtained from 6 subjects over a period of 180 min after  $^{68}\text{Ga}$ -citrate administration. Figure 2 shows representative images from a subject. The radioactivity concentrations in 20 organs or tissues of interest

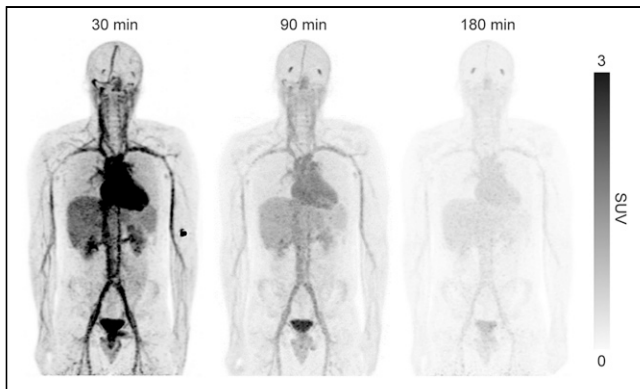


**FIGURE 2.** Whole-body distribution of 195 MBq of  $^{68}\text{Ga}$ -citrate in healthy 22-y-old man (73 kg).

were quantified at time points of 1, 5, 10, 20, 30, 90, and 180 min, and the results are presented in Supplemental Table 2. At 30 min after injection, SUVs in the brain, heart contents, kidneys, liver, trabecular bone, and red marrow were  $0.26 \pm 0.04$  (mean  $\pm$  SD),  $5.16 \pm 0.48$ ,  $3.15 \pm 0.46$ ,  $2.78 \pm 0.25$ ,  $0.70 \pm 0.15$ , and  $1.80 \pm 0.12$ , respectively. Figure 3 shows time-activity curves for the 20 organs or tissues, revealing the whole-body distribution kinetics of radioactivity over the 180 min after  $^{68}\text{Ga}$ -citrate administration.

The mean voided radioactivity at a mean void time of 61 min after injection (during a break between PET imaging session) was  $1.76 \pm 0.47$  percentage injected dose (Fig. 4). All 6 subjects were able to urinate during the first PET imaging session break, 3 were able to urinate between imaging session 2 and 3, and 2 after the complete imaging session.

Radioactivity clearance from the blood was slow (Fig. 5). The  $C_0$  in SUV units was  $17.3 \pm 1.8$  g/mL (Supplemental Table 3). The inverse of  $C_0$ , which is related to the total plasma volume, was  $0.059 \pm 0.006$  L/kg. The plasma concentration at 4 h ( $n = 5$ ) was  $5.8 \pm 0.6$  g/mL, and its inverse, which may be related to the extracellular volume of the body, was  $0.17 \pm 0.02$  L/kg.

### Residence Times and Radiation Dose Estimates

The residence times (normalized numbers of disintegrations) were determined for the source organs and the remainder of the body of each subject, and their mean  $\pm$  SD, range, and coefficient of variation are listed in Table 1. The coefficients of variation were in the range of 4%–49%. The largest residence times were in muscle ( $0.365 \pm 0.043$  h), liver ( $0.091 \pm 0.017$  h), lungs ( $0.079 \pm 0.008$  h), and heart contents ( $0.048 \pm 0.006$  h).

The organ dose estimates (Table 2) were calculated for a 70-kg adult man. The organs with the highest doses were the heart wall ( $0.077 \pm 0.008$  mSv/MBq), urinary bladder wall ( $0.039 \pm 0.010$  mSv/MBq), kidneys ( $0.036 \pm 0.004$  mSv/MBq), and lungs ( $0.036 \pm 0.003$  mSv/MBq). The lowest dose was in the brain ( $0.004 \pm 0.001$  mSv/MBq). The mean effective dose (International Commission on Radiological Protection publication 103) (20) was  $0.021 \pm 0.001$  mSv/MBq. Thus, the effective dose from 200 MBq of injected radioactivity of  $^{68}\text{Ga}$ -citrate was 4.2 mSv.

Organ dose estimates according to OLINDA 1.0 are presented in Supplemental Table 4.

### DISCUSSION

We previously studied  $^{68}\text{Ga}$ -citrate in experimental disease models, as well as in patients with infections (8,15,21). The

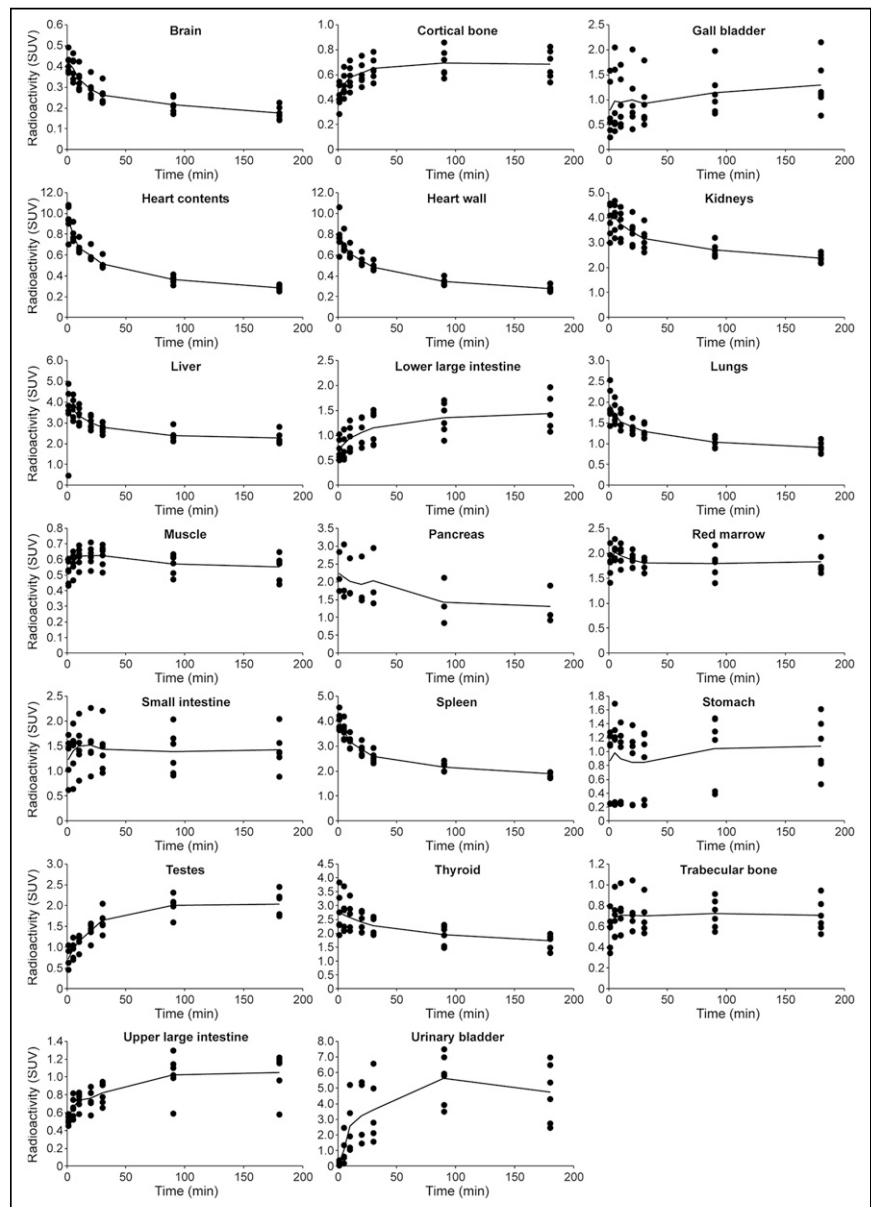


**FIGURE 3.** Time-activity curves of main organs. Circles represent each individual, and line is average.

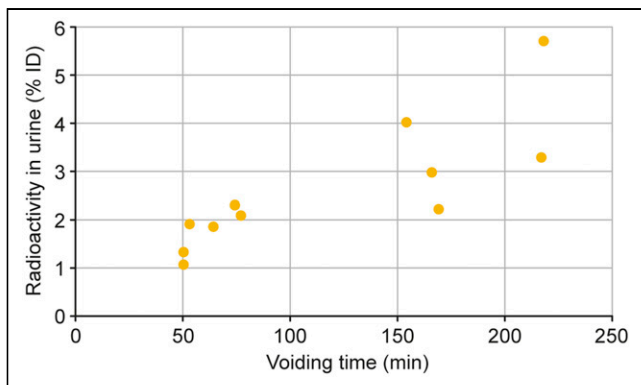


**FIGURE 4.** Percentage of injected  $^{68}\text{Ga}$ -citrate radioactivity dose (%ID) in urine as function of time.

current study was a basic investigation in healthy humans to collect data on whole-body distribution kinetics and radiation dose estimates, which will be useful in planning future clinical trials with  $^{68}\text{Ga}$ -citrate.

#### Preparation of $^{68}\text{Ga}$ -Citrate

The radiopharmaceutical  $^{68}\text{Ga}$ -citrate was produced using a straightforward protocol (3). The acetone-based cation-exchange cartridge elution method is an effective option for concentrating  $^{68}\text{Ga}$  radioactivity eluted from a generator (1). In our hospital, this method is used to manufacture 3 radiopharmaceuticals, including  $^{68}\text{Ga}$ -citrate, in a fully automated manner. Citrate is a natural ligand that can coordinate some metal ions, including gallium. Because of the nature of the nuclear physics of  $^{68}\text{Ga}$ , the molarity of  $^{68}\text{Ga}$  in a batch of eluate from a  $^{68}\text{Ge}/^{68}\text{Ga}$  generator is tiny. By contrast, the molarity of citrate (0.14 mmol) is in great excess to ensure efficient coordination, which is neither feasible nor typical in the production of many other  $^{68}\text{Ga}$ -radiopharmaceuticals. In this sense, citrate acts also as a vehicle, in addition to its role as a chelator. On instant thin-layer chromatography, the chromatography behaviors of  $^{68}\text{Ga}$ -citrate and free  $^{68}\text{Ga}$  show a clear difference (Fig. 1B); free  $^{68}\text{Ga}$  remains at the baseline whereas  $^{68}\text{Ga}$ -citrate migrates up on the instant thin-layer chromatography, with a retention factor of 0.93. As there is not a citrate dose limit set in the European Pharmacopoeia; quantification of the citrate in the end-product formulation is not relevant in the quality control procedure.

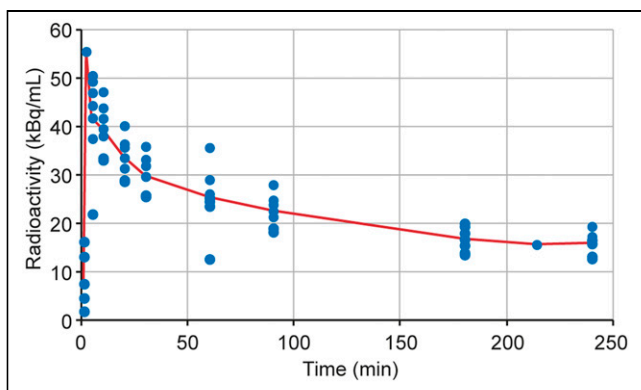


**FIGURE 5.** Concentration of radioactivity in arterialized venous plasma as function of time after  $^{68}\text{Ga}$ -citrate injection. Dots represent each individual, and line is average.

**TABLE 1**  
Residence Times (Hours) in Source Organs After Injection of  $^{68}\text{Ga}$ -Citrate

Organ	Mean $\pm$ SD	COV (%)	Range
Brain	0.008 $\pm$ 0.001	19	0.006–0.009
Gallbladder contents	0.000 $\pm$ 0.000	48	0.000–0.001
Left colon	0.002 $\pm$ 0.001	23	0.001–0.003
Small intestine	0.012 $\pm$ 0.003	27	0.007–0.016
Stomach contents	0.009 $\pm$ 0.004	38	0.004–0.013
Right colon	0.002 $\pm$ 0.001	23	0.001–0.003
Rectum	0.002 $\pm$ 0.001	25	0.001–0.003
Heart contents	0.048 $\pm$ 0.006	12	0.041–0.055
Heart wall	0.027 $\pm$ 0.004	13	0.024–0.033
Kidneys	0.020 $\pm$ 0.003	14	0.017–0.023
Liver	0.091 $\pm$ 0.017	19	0.077–0.121
Lungs	0.079 $\pm$ 0.008	10	0.066–0.088
Muscle	0.365 $\pm$ 0.043	12	0.299–0.420
Pancreas	0.005 $\pm$ 0.002	49	0.003–0.008
Red marrow	0.046 $\pm$ 0.004	10	0.038–0.052
Cortical bone	0.032 $\pm$ 0.005	15	0.026–0.040
Trabecular bone	0.009 $\pm$ 0.002	22	0.007–0.012
Spleen	0.009 $\pm$ 0.002	28	0.006–0.012
Testes	0.002 $\pm$ 0.000	15	0.001–0.002
Thyroid	0.001 $\pm$ 0.000	19	0.000–0.001
Urinary bladder contents	0.021 $\pm$ 0.008	37	0.013–0.035
Remainder of body	0.810 $\pm$ 0.033	4	0.767–0.858

COV = coefficient of variation (SD/mean  $\times$  100).

#### PET Imaging and Biodistribution

In a typical  $^{68}\text{Ga}$ -radiopharmaceutical, the  $^{68}\text{Ga}$ -radionuclide is attached to a targeting molecule, such as a peptide, and the targeting molecule takes the radioactivity to the specific organs and tissues to be imaged. In the case of  $^{68}\text{Ga}$ -citrate, the imaging and biodistribution are most probably based on the biologic mechanisms of  $^{68}\text{Ga}^{3+}$ , which can be chelated in vivo with biomolecules, including ferritins (13). This implies that in vivo transmetalation takes place, even though citrate has sufficient strength to coordinate  $^{68}\text{Ga}^{3+}$  in the manufacturing procedures. However, comparison studies have indicated that the imaging performance of  $^{68}\text{Ga}$ -citrate is better than that of intravenously injected  $^{68}\text{Ga}$ -chloride, at least as far as the limited available evidence shows (15), which might be an indication that citrate plays a role as a vehicle in the in vivo biodistribution. In this study, particular care was taken to ensure that the  $^{68}\text{Ga}$ -citrate injection did not involve any gallium colloids, which usually accompany the  $^{68}\text{Ge}/^{68}\text{Ga}$  generator eluate or are formed if injected as  $^{68}\text{Ga}$ -chloride.

For the PET imaging, each subject was intravenously administered  $204 \pm 8$  MBq of  $^{68}\text{Ga}$ -citrate. In a routine PET procedure performed in our hospital, such as one using the standard tracer  $^{18}\text{F}$ -FDG, the typical radioactivity dose is 4 MBq/kg of body weight. In this study, we used  $204 \pm 8$  MBq ( $2.7 \pm 0.2$  MBq/kg)

**TABLE 2**  
Organ Doses and Effective Doses (mSv/MBq) After  
Injection of <sup>68</sup>Ga-Citrate

Organ	Mean ± SD	COV (%)	Range
Adrenals	0.019 ± 0.001	4	0.018–0.020
Brain	0.004 ± 0.001	12	0.004–0.005
Breasts	0.013 ± 0.000	2	0.012–0.013
Colon, left	0.021 ± 0.002	7	0.019–0.023
Colon, right	0.017 ± 0.001	4	0.016–0.018
Esophagus	0.015 ± 0.000	2	0.015–0.016
Eyes	0.011 ± 0.000	3	0.010–0.011
Gallbladder wall	0.017 ± 0.001	6	0.016–0.019
Heart wall	0.077 ± 0.008	11	0.067–0.087
Kidneys	0.036 ± 0.004	12	0.031–0.041
Liver	0.033 ± 0.005	16	0.029–0.043
Lungs	0.036 ± 0.003	8	0.031–0.040
Osteogenic cells	0.017 ± 0.001	6	0.015–0.018
Pancreas	0.020 ± 0.007	36	0.015–0.034
Prostate	0.013 ± 0.000	2	0.012–0.013
Rectum	0.020 ± 0.001	7	0.018–0.022
Red marrow	0.020 ± 0.001	5	0.019–0.022
Salivary glands	0.012 ± 0.000	3	0.011–0.012
Small intestine	0.022 ± 0.002	11	0.019–0.025
Spleen	0.032 ± 0.007	23	0.025–0.044
Stomach wall	0.024 ± 0.004	15	0.018–0.027
Testes	0.022 ± 0.003	13	0.019–0.026
Thymus	0.016 ± 0.000	2	0.016–0.017
Thyroid	0.017 ± 0.002	14	0.014–0.021
Urinary bladder wall	0.039 ± 0.010	26	0.029–0.057
Total body	0.015 ± 0.000	1	0.014–0.015
Effective dose, ICRP 60 (27)	0.023 ± 0.001	3	0.021–0.023
Effective dose, ICRP 103 (20)	0.021 ± 0.001	3	0.020–0.022

COV = coefficient of variation (SD/mean × 100); ICRP = International Commission on Radiological Protection.

of <sup>68</sup>Ga-citrate per subject, which is in the typical dose range of our <sup>68</sup>Ga-radiopharmaceutical PET studies. The mass of gallium injected was negligible. It is noteworthy that when gallium is administered as a drug in high doses, the biodistribution is known to change (22,23).

The sequential whole-body imaging was performed for 180 min to monitor the tracer kinetics in vivo. For visualization purposes, we prepared representative PET/CT images from a 22-y-old man and scaled the SUVs from 1 to 3 (Fig. 2). These images clearly show that the radioactivity concentration was much higher in heart, liver, lungs, and kidneys than in other organs. At 180 min after injection, the whole-body radioactivity concentration became very low, an indication of a sufficient data collection time range. To further quantify the radioactivity concentration in the 20 organs of

interest, time–activity curves were drawn from 0 to 180 min after administration (Fig. 3). Among the organs and tissues, the time–activity curves from gallbladder, lower large intestine (left colon and rectum), testes, and upper large intestine (right colon) were still increasing slightly at 180 min. It was not clear what factors might have caused the slight accumulations in these organs. In cortical bone, red marrow, small intestine, and trabecular bone, the time–activity curves showed a steady radioactivity residence along with time. In the urinary bladder, the general trend of radioactivity development was an initial increase and then a decrease. In the rest of the organs, the time–activity curves decreased to varying extents over the period.

The radioactivity concentration in plasma stayed at a high level (Fig. 5), similar to that reported previously for the <sup>68</sup>Ge/<sup>68</sup>Ga generator eluate <sup>68</sup>Ga-chloride in a study on rats (24); the slow decrease at 3–4 h prevents reliable estimation of the total area under the curve (from time zero to infinity) and total clearance. In previous animal studies, we found that the in vivo kinetics of <sup>68</sup>Ga-citrate and <sup>68</sup>Ga-chloride differed, possibly because the chelating properties of citrate prevent the precipitation of <sup>68</sup>Ga(OH)<sub>3</sub> (15).

#### Radiation Dose Estimates

To determine the radiation burden, we analyzed the kinetics of radioactivity concentration in the main organs of healthy men up to 3 h after an intravenous bolus injection of <sup>68</sup>Ga-citrate. In addition to the SD and range, the coefficient of variation was used to indicate the precision and repeatability of the measurements among the 6 subjects. Our results revealed that the heart wall received the highest radiation dose, followed by the urinary bladder wall. This may be partially due to the relatively slow blood clearance and urinary excretion as the main clearance route. However, the relatively slow blood clearance was not a problem for target visualization in previous studies. The organ with the lowest radiation exposure was the brain (0.004 ± 0.001 mSv/MBq). Overall, the effective dose of <sup>68</sup>Ga-citrate (0.021 ± 0.001 mSv/MBq) was comparable to that of widely used PET tracers, including <sup>68</sup>Ga-DOTANOC (0.025 mSv/MBq) (25) and <sup>18</sup>F-FDG (0.019 mSv/MBq) (26). For example, a 200-MBq dose of <sup>68</sup>Ga-citrate may result in an effective dose of 4.2 ± 0.2 mSv.

#### CONCLUSION

The radiation burden from administration of <sup>68</sup>Ga-citrate for PET imaging is comparable to that of other commonly used <sup>68</sup>Ga-radiopharmaceuticals. The low radiation exposure of <sup>68</sup>Ga-citrate would allow for studies with multiple scans in the same individuals over the course of a year.

#### DISCLOSURE

The study was conducted within the Finnish Centre of Excellence in Cardiovascular and Metabolic Diseases, supported by the Academy of Finland, University of Turku, Turku University Hospital, and Åbo Akademi University. The study was financially supported by grants from the State Research Funding of Turku University Hospital and the Sigrid Jusélius Foundation. No other potential conflict of interest relevant to this article was reported.

#### ACKNOWLEDGMENTS

We thank the technical and nursing staff at Turku PET Centre for their assistance in this work, and we thank Timo Kattelus for preparing figures.

## KEY POINTS

**QUESTION:** What are the distribution kinetics of  $^{68}\text{Ga}$ -citrate in healthy humans, and what is the radiation burden resulting from its administration?

**PERTINENT FINDINGS:** Six healthy men underwent dynamic whole-body PET/CT imaging with blood and urine measurements.  $^{68}\text{Ga}$ -citrate showed slow clearance from the blood circulation through renal excretion. The highest radiation exposure was to the heart wall. The effective dose of 0.021 mSv/MBq is similar to that of other commonly used  $^{68}\text{Ga}$  tracers.

**IMPLICATIONS FOR PATIENT CARE:** The characteristics of  $^{68}\text{Ga}$ -citrate are favorable for human studies involving multiple scans in the same subject over the course of a year.

## REFERENCES

- Käkelä M, Luoto P, Viljanen T, et al. Adventures in radiosynthesis of clinical grade [ $^{68}\text{Ga}$ ]Ga-DOTA-Siglec-9. *RSC Advances*. 2018;8:8051–8056.
- Mintun MA, Dennis DR, Welch MJ, Mathias CJ, Schuster DP. Measurements of pulmonary vascular permeability with PET and gallium-68 transferrin. *J Nucl Med*. 1987;28:1704–1716.
- Rizzello A, Pierro DD, Lodi F, et al. Synthesis and quality control of  $^{68}\text{Ga}$  citrate for routine clinical PET. *Nucl Med Commun*. 2009;30:542–545.
- Nanni C, Errani C, Boriani L, et al.  $^{68}\text{Ga}$ -citrate PET/CT for evaluating patients with infections of the bone: preliminary results. *J Nucl Med*. 2010;51:1932–1936.
- Kumar V, Boddeti DK, Evans SG, Angelides S.  $^{68}\text{Ga}$ -citrate-PET for diagnostic imaging of infection in rats and for intra-abdominal infection in a patient. *Curr Radiopharm*. 2012;5:71–75.
- Vorster M, Maes A, Jacobs A, et al. Evaluating the possible role of  $^{68}\text{Ga}$ -citrate PET/CT in the characterization of indeterminate lung lesions. *Ann Nucl Med*. 2014;28:523–530.
- Behr SC, Aggarwal R, Seo Y, et al. A feasibility study showing [ $^{68}\text{Ga}$ ]citrate PET detects prostate cancer. *Mol Imaging Biol*. 2016;18:946–951.
- Salomäki SP, Kemppainen J, Hohenthal U, et al. Head-to-head comparison of  $^{68}\text{Ga}$ -citrate and  $^{18}\text{F}$ -FDG PET/CT for detection of infectious foci in patients with *Staphylococcus aureus* bacteraemia. *Contrast Media Mol Imaging*. 2017;2017:3179607.
- Aggarwal R, Behr SC, Paris PL, et al. Real-time transferrin-based PET detects MYC-positive prostate cancer. *Mol Cancer Res*. 2017;15:1221–1229.
- Aparici CM, Behr SC, Seo Y, et al. Imaging hepatocellular carcinoma with  $^{68}\text{Ga}$ -citrate PET: first clinical experience. *Mol Imaging*. 2017;16:1536012117723256.
- Behr SC, Villanueva-Meyer JE, Li Y, et al. Targeting iron metabolism in high-grade glioma with  $^{68}\text{Ga}$ -citrate PET/MR. *JCI Insight*. 2018;3:e93999.
- Tseng JR, Chang YH, Yang LY, et al. Potential usefulness of  $^{68}\text{Ga}$ -citrate PET/CT in detecting infected lower limb prostheses. *EJNMMI Res*. 2019;9:2.
- Xu T, Chen Y. Research progress of [ $^{68}\text{Ga}$ ]citrate PET's utility in infection and inflammation imaging: a review. *Mol Imaging Biol*. 2020;22:22–32.
- Nielsen OL, Afzelius P, Bender D, et al. Comparison of autologous  $^{111}\text{In}$ -leukocytes,  $^{18}\text{F}$ -FDG,  $^{11}\text{C}$ -methionine,  $^{11}\text{C}$ -PK11195 and  $^{68}\text{Ga}$ -citrate for diagnostic nuclear imaging in a juvenile porcine haematogenous *Staphylococcus aureus* model. *Am J Nucl Med Mol Imaging*. 2015;5:169–182.
- Lankinen P, Noponen T, Autio A, et al. A comparative  $^{68}\text{Ga}$ -citrate and  $^{68}\text{Ga}$ -chloride PET/CT imaging of *Staphylococcus aureus* osteomyelitis in the rat tibia. *Contrast Media Mol Imaging*. 2018;2018:9892604.
- Bettinardi V, Presotto L, Rapisarda E, Picchio L, Gianolli L, Gilardi MC. Physical performance of the new hybrid PET/CT Discovery-690. *Med Phys*. 2011;38:5394–5411.
- International Commission on Radiological Protection. Basic anatomical and physiological data for use in radiological protection: reference values. *ICRP Publication 89*. Pergamon Press; 2002.
- Thomas SR, Stabin MG, Chin-Tu C, Samarungta RC. MIRD pamphlet no. 14 revised: a dynamic urinary bladder model for radiation dose calculations. *J Nucl Med*. 1999;40(suppl):102S–123S.
- Siegel JA, Thomas SR, Stubbs JB, et al. MIRD pamphlet no. 16: techniques for quantitative radiopharmaceutical biodistribution data acquisition and analysis for use in human radiation dose estimates. *J Nucl Med*. 1999;40(suppl):37S–61S.
- ICRP publication 103: the 2007 recommendations of the International Commission on Radiological Protection. *Ann ICRP*. 2007;37:1–332.
- Aro E, Seppänen M, Mäkelä KT, Luoto P, Roivainen A, Aro HT. PET/CT to detect adverse reactions to metal debris in patients with metal-on-metal hip arthroplasty: an exploratory prospective study. *Clin Physiol Funct Imaging*. 2018;38:847–855.
- Bernstein LR. Mechanisms of therapeutic activity for gallium. *Pharmacol Rev*. 1998;50:665–682.
- AR-501 (gallium citrate): novel anti-infective for the growing problem of antibiotic resistance. Ardis Pharmaceuticals website. <https://www.aridispharma.com/ar-501/>. Accessed July 20, 2022.
- Autio A, Virtanen H, Tolvanen T, et al. Absorption, distribution and excretion of intravenously injected  $^{68}\text{Ge}/^{68}\text{Ga}$  generator eluate in healthy rats, and estimation of human radiation dosimetry. *EJNMMI Res*. 2015;5:117.
- Pettinato C, Sarnelli A, Di Donna M, et al.  $^{68}\text{Ga}$ -DOTANOC: biodistribution and dosimetry in patients affected by neuroendocrine tumors. *Eur J Nucl Med Mol Imaging*. 2008;35:72–79.
- ICRP publication 80: recalculated dose data for 19 frequently used radiopharmaceuticals from ICRP publication 53. *Ann ICRP*. 1998;28:47–83.
- ICRP publication 60: recommendation of the International Commission on Radiological Protection. *Ann ICRP*. 1991;21:493–502.